Surface structure of ultrathin smectic films on silicon substrates: Pores and islands

Benjamin Schulz* and Christian Bahr†

Max Planck Institute for Dynamics and Self-Organization, Bunsenstraße 10, D-37073 Göttingen, Germany

(Received 4 February 2011; published 27 April 2011)

We present an atomic force microscopy (AFM) and ellipsometry study of ultrathin smectic films on silicon substrates. By controlling the amount of the liquid-crystal material that is spin coated on the substrate, we are able to prepare films consisting of a defined small number (ranging from 1 to 4) of smectic layers. AFM measurements show that the films possess a specific surface structure with a lateral feature size of a few microns and steplike height variations of 3.3 nm. The height of the steps corresponds to the smectic layer spacing of the material used, indicating that the surface structure is the result of a partial formation of the topmost smectic layer of these films. The pattern of the surface structure either corresponds to isolated islands (regions in which the film thickness is enhanced by one smectic layer) or consists of pores (film thickness decreased by one layer). A smooth surface is only obtained if the amount of the liquid-crystal material is precisely tuned to certain values, indicating the formation of a complete smectic top layer. A well-defined relation exists between the liquid crystal concentration in the spin-coating solution and the obtained structure, enabling the controlled generation of island structures, pore structures, or smooth surfaces. The two-dimensional island or pore structure is stable on the time scale of a few days. Preliminary results concerning the thermal stability are reported. Our study highlights the usefulness of AFM measurements for the study of smectic liquid-crystal surfaces.

DOI: 10.1103/PhysRevE.83.041710 PACS number(s): 61.30.Hn, 61.30.Jf, 68.15.+e

I. INTRODUCTION

Thin films and surfaces of liquid crystals are important from both fundamental (e.g., for the study of phase transitions in two-dimensional systems) and applied viewpoints (e.g., the anchoring of liquid-crystal molecules on solid substrates is essential for the performance of liquid-crystal displays). The smectic-A liquid-crystal phase is an orientationally ordered fluid in which the rodlike molecules align along a common direction, designated by a unit vector $\vec{n}$, and arrange themselves in layers with the layer normal being parallel to $\vec{n}$. Thin smectic-A films, consisting of only a small number of layers, have been studied in various configurations: as freely suspended films, as Langmuir films on a water surface, and as films on a solid substrate.

Freely suspended films, which are spanned on a solid frame, consist of an integer number of molecular smectic layers that are perfectly parallel to the two free surfaces. When the area of a film is increased by an expansion of the frame, "pores" appear in the film, i.e., circular areas in which the film thickness is one or several layers smaller than the initial thickness. If the film area is decreased by a compression of the frame, "islands" appear, which are circular areas possessing a larger film thickness [1]. When the change of the film area is stopped, the generated pores or islands expand or shrink until the film thickness is again homogeneous throughout the film; this behavior occurs because the film can exchange material with its meniscus, which acts as a reservoir. From the dynamics of these processes, the line tension of the domain boundaries (edge dislocations) separating regions of different film thickness can be determined [2,3].

A similar formation of islands and pores can be observed in smectic-A films that are prepared as Langmuir films on a water surface [4–7]. Islands are generated by a compression of the film, and pores form if a multilayer film is expanded. In contrast to freely suspended films, domains of different film thickness can coexist under static conditions on long time scales since Langmuir films are not connected to a reservoir of liquid-crystal bulk material. However, due to the fluid nature of the film and the substrate, islands are mobile and do eventually coalesce. The islands can be deformed, and from their relaxation back to a circular shape the line tension of the corresponding edge dislocation can be determined [8]. With ongoing compression of the film area, islands merge to complete smectic layers, and multilayer films are formed.

Thin smectic films on solid substrates have been formed by various methods: thermal evaporation [9–13], spin coating [14–18], spreading of small droplets [19–23], and transferring freely suspended films [24–26] and Langmuir films [10,12,25]. Compared to freely suspended and Langmuir films, it appears more difficult to form homogeneous films on solid substrates. Depending on the liquid crystal and the substrate material, films deposited by evaporation often show dewetting [10]. Transferred freely suspended and Langmuir films reveal thickness steps and pores when studied by atomic force microscopy (AFM) [25,26]. Smectic films with a thickness of a few hundred nanometers, prepared by spin coating onto crystalline substrates, have been studied by optical microscopy, x-ray diffraction, and AFM measurements [17]. In these thicker films, antagonistic anchoring conditions of the liquid-crystal molecules at the two film interfaces lead to an elastic bend deformation of the smectic layers. Ultrathin smectic films prepared by spin coating have been studied by x-ray reflectivity [14,27,28], which enables a simultaneous determination of film thickness h and smectic layer spacing d. The thickness of these films was between very few (2 or 3) and ≈35 smectic layers. The x-ray reflectivity data indicated that these thin films can be seen as stacks of smectic layers that lie flat on the substrate. However, in several cases a noninteger value of the ratio h/d was obtained, which was attributed to a certain

*benjamin.schulz@ds.mpg.de
†christian.bahr@ds.mpg.de

 ©2011 American Physical Society

roughness, but the detailed surface structure of the films was not clarified. We present here an AFM and ellipsometry study of similar ultrathin smectic films.

We use a spin-coating technique to prepare ultrathin smectic films on a silicon substrate under conditions where the amount of liquid-crystal material is sufficient only for a few molecular layers. Accordingly, we obtain smectic films consisting of a small defined number of layers (in the range between one and four layers). Our AFM measurements show that the films possess a specific surface structure: Unless the amount of the liquid-crystal material is precisely tuned, the topmost layer is formed only partially; i.e., either it is fragmented into isolated islands, or it shows a porous structure. We find a well-defined relation between the liquid-crystal concentration in the spin-coating solution and the resulting film structure; i.e., one can determine whether the film surface will have a smooth, a porous, or an island structure. The AFM data indicate that the thickness steps at the surface correspond to the thickness of a single smectic layer, which is, for the material under investigation, a molecular bilayer. The ellipsometry data confirm the structure resulting from the AFM measurements.

II. EXPERIMENT

We prepared thin films of the standard mesogen 4-*n*-octyl-4′-cyanobiphenyl (8CB, SYNTHON Chemicals), which has a transition from crystalline to smectic-*A* at 21.5 °C, from smectic-*A* to nematic at 33.7 °C, and from nematic to isotropic liquid at 40.5 °C. The liquid crystal was dissolved in toluene (Merck, 99.9%) in a defined concentration. The films were spin coated on silicon substrates covered with a native oxide layer at a spin speed of 6000 rpm. The spin-coating time was 30 s, with additional 1 s for acceleration and 5 s for deceleration. Before use, all substrates were cleaned using piranha solution (60% sulfuric acid, 40% hydrogen peroxide, both Sigma-Aldrich). Different film thicknesses were obtained by changing the concentration of the liquid crystal in toluene in a range of 0.2–5.0 mg/ml.

The surface of the films was imaged using an AFM (Veeco diMultiMode) in noncontact mode, in which the sample surface is probed by a cantilever (Olympus AC240-TS) oscillating at a frequency slightly below its resonance frequency. The cantilevers had a spring constant of around 2 N/m. When working with constant damping of the tip, one is able to image the topology of a surface. Most AFM results were obtained at ambient temperature; some measurements were conducted at elevated temperatures using a multimode temperature control unit. More details on AFM measurements of smectic films can be found in [29].

A home-built phase-modulated ellipsometer [30] was used to determine the total thickness of the films. The ellipsometer determines the magnitude $\tan\Psi$ and the argument Δ of the complex amplitude ratio $r_p/r_s = \tan\Psi \exp(i\Delta)$ of the *p*- and *s*-polarized components of a laser beam ($\lambda = 633$ nm) that is reflected from the liquid-crystal-film–substrate system. The quantities $\tan\Psi$ and Δ are measured as a function of the angle of incidence θ_i within an interval of a few degrees broad around the Brewster angle θ_B. For $\theta_i = \theta_B$ (which is achieved if $\Delta = \pi/2$), the magnitude of $\tan\Psi$ is nearly linearly related to the film thickness h. The quantitative determination of h from the ellipsometric data is described in the following section.

III. RESULTS AND DISCUSSION

We prepared films by spin coating from 8CB solutions in toluene with concentrations c from 0.2 to 5 mg/ml in steps of 0.2 mg/ml. All prepared films were studied by AFM and ellipsometric measurements. Whereas the films looked homogeneous in an optical microscope, the high resolution of the AFM measurements revealed a special surface structure of the films with a lateral feature size of a few microns and steplike height variations of ≈3 nm. In most cases, the AFM images show a porouslike surface; i.e., a number of regions with sometimes nearly circular and sometimes more irregular boundaries are observed in which the thickness is smaller compared to the rest of the film. Less frequently, the film surfaces show an island structure, i.e., regions possessing a higher film thickness. For a few certain concentrations, the films had an almost smooth surface, with only a few irregularities. These concentrations amounted approximately to 1.8, 2.8, 3.8, and 4.8 mg/ml. It is reasonable to assume that, for these concentrations, films consisting of one, two, three, and four complete smectic layers are formed, whereas, for the other concentrations, films with an incomplete top layer are obtained. Ellipsometric measurements of the film thickness, which will be described in the second part of this section, confirm this assumption. We should point out that all the prepared films show a homogeneous structure throughout the whole substrate area (≈0.5 cm^2): if AFM images are recorded in different areas of a given film, the same surface structure is obtained, and the results of the ellipsometry measurements do not vary if the measurements are conducted in different regions of a given film. We first discuss our AFM results in more detail.

Figure 1 shows a sequence of AFM images of the surface topography of films prepared in the concentration range 2.8 mg/ml $\leqslant c \leqslant$ 3.8 mg/ml. For $c = 2.8$ mg/ml, we observe an essentially smooth surface with a small number of islands.

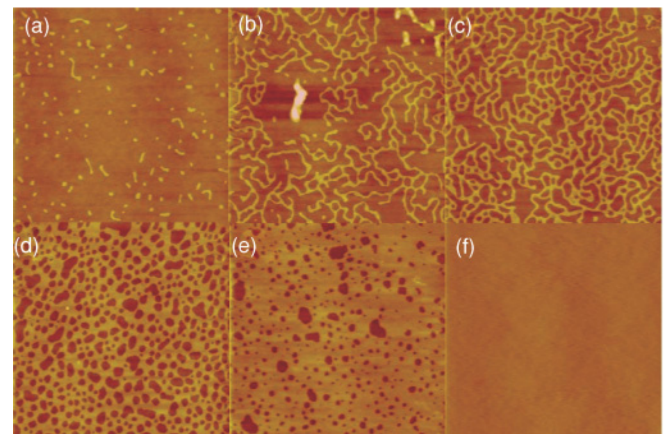

FIG. 1. (Color online) AFM height images of spin-coated 8CB films on silicon wafers. The 8CB concentration in the spin-coating solution was (a) 2.8 mg/ml, (b) 3.0 mg/ml, (c) 3.2 mg/ml, (d) 3.4 mg/ml, (e) 3.6 mg/ml, and (f) 3.8 mg/ml. Each image shows an area of 20 × 20 μm^2.

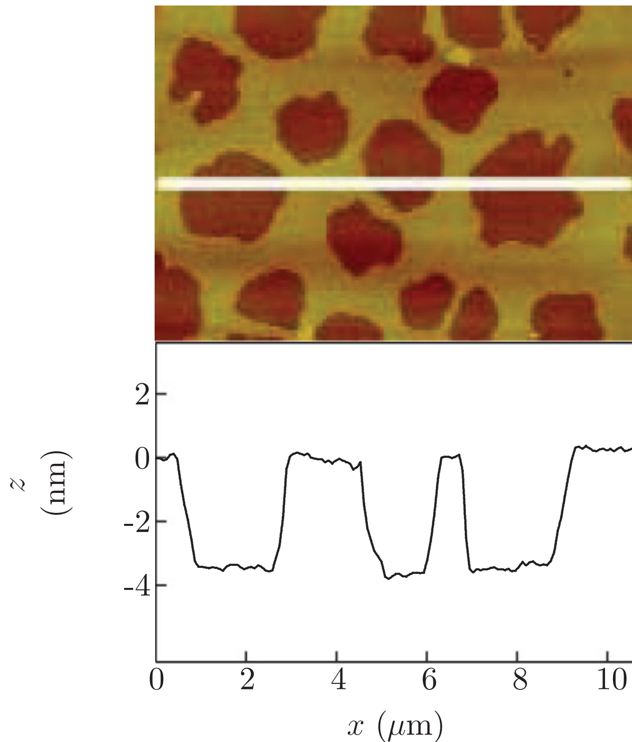

FIG. 2. (Color online) (top) AFM height image (10 × 7 μm^2) of a film prepared with a 3.4 mg/ml solution. (bottom) Cross section along the white line in the above AFM image demonstrating the thickness step height of 3.3 ± 0.2 nm.

With increasing concentration, the islands grow (3.0 mg/ml) and merge to a porous structure (3.2 mg/ml). A further increase of the concentration results in a decrease of the size of the pores (3.4–3.6 mg/ml) until a smooth surface is again obtained for $c = 3.8$ mg/ml. Exactly the same sequence of changes in the surface topography is obtained for the concentration intervals between 1.8 and 2.8 mg/ml and between 3.8 and 4.8 mg/ml; i.e., without additional information, it would not be possible to decide if an AFM image of a film surface was obtained for, e.g., a film prepared from a 2.5 mg/ml solution or from a 3.5 mg/ml solution. Figure 2 shows a cross section through a film prepared with a 3.4 mg/ml solution. The thickness step at the edge of the islands or pores amounts to 3.3 ± 0.2 nm, which coincides well with the smectic layer spacing of 8CB as determined by x-ray studies (3.16 nm [31]). The volume smectic phase of 8CB is of the smectic-A_d type; i.e., each smectic layer is a molecular bilayer in which the polar molecules adopt an antiparallel, partially interdigitating arrangement [32]. When we use the term “smectic layer” in the following, we always mean the bilayer structure observed in the smectic volume phase of 8CB. The measured magnitude of the thickness step depends only slightly on the scanning parameters, and we can conclude that, in the concentration range above 1.8 mg/ml, where the substrate is covered by at least one complete smectic layer, the island or pore structure at the film surface results from a partial formation of the topmost smectic layer of the film.

The behavior in the concentration range below 1.8 mg/ml differs by a few aspects: The amount of material that is needed for the formation of the first complete film is obviously larger than in the range above 1.8 mg/ml (where a concentration increase of ≈1 mg/ml is sufficient for the formation of one additional layer). AFM images of films obtained with $c = 0.4$ mg/ml or less show smooth surfaces without structural features. The first islands are observed for $c = 0.6$ mg/ml; for $c > 0.8$ mg/ml, a pore structure is found, and a concentration of 1.7–1.8 mg/ml is necessary to obtain a complete film without pores. The larger amount of material needed for the first complete film is the result of a special structure formed by 8CB molecules in contact with substrates possessing planar anchoring conditions like the silicon wafers of our study. On a planar anchoring substrate, the 8CB molecules prefer to align parallel to the substrate plane, whereas at the interface to air the molecules adopt a perpendicular alignment. In thicker 8CB films (hundreds of nanometers or more) on planar anchoring substrates, the antagonistic anchoring conditions are reconciled by an elastic deformation of the smectic layers. In ultrathin smectic films, the energy of such a layer deformation would be too large, and a special trilayer structure is formed, which consists of a tilted polar molecular monolayer, which is in direct contact with the substrate, and one molecular bilayer, i.e., a single smectic layer, on top of the monolayer. This trilayer structure, which has been observed for Langmuir films on water [5] as well as for evaporated films [13] and precursor films in spreading experiments on silicon [19–21], is likely to exist also in our experiment. Thus, for the formation of the first complete film an amount of material for roughly 1.5 smectic layers would be needed. In this context, it would be important to determine the magnitude of the thickness steps of the pores and islands of the films obtained in this concentration range. For the thickness of the trilayer structure, values between 4.1 and 4.5 nm have been determined [19–21]; thus, one would expect a step height clearly above the value obtained for the thicker films (3.3 nm). Unfortunately, the measured value of the step height in these thin films depends more strongly on the scanning parameters than in the films obtained with $c \geqslant 1.8$ mg/ml. Similar to the results of Bardon *et al.* [33], we observe that the apparent step height increases with decreasing value of the damping ratio A_d/A_f (where A_f is the oscillation amplitude of the free tip and A_d is the amplitude of the damped oscillation during the measurement). An extrapolation of our data to $A_d/A_f \to 1$ indicates that the step height in the thin films also amounts to ≈3 nm, suggesting that the ground of a pore does not consist of the bare silicon substrate but is covered by the tilted monolayer of 8CB molecules. Thus, apart from the observation that for the preparation of the complete first film a larger amount of material is needed compared to the following complete films, our AFM measurements do not give further information about the structure of this complete first film or the presence of a tilted monolayer on the substrate surface. However, ellipsometric thickness measurements, which will be described in detail at the end of this section, yield a thickness of 4.5 nm for this first complete film. This result is a strong indication that the trilayer structure, which has been observed in the earlier experiments [5,13,19–21], is also present in our 8CB films.

Another aspect in which these ultrathin films ($c <$ 1.8 mg/ml) differ from the thicker films becomes obvious when we regard the phase data of the AFM measurements. Figure 3 shows the difference $\Delta\phi$ between the phase values

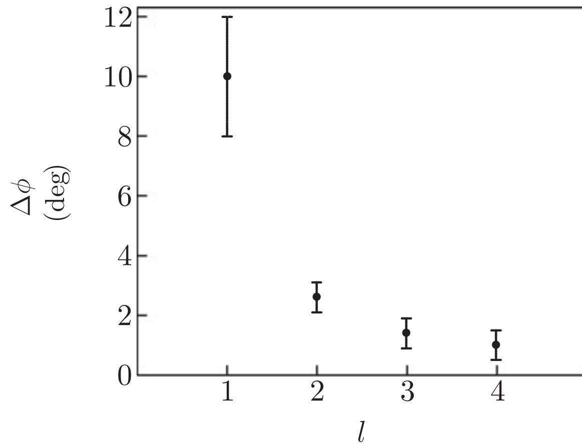

FIG. 3. Difference $\Delta\phi$ between the AFM phase data obtained for the thicker (film thickness l smectic layers) and the thinner areas (film thickness $l-1$ smectic layers) of the films; the $\Delta\phi$ data were determined for a larger number of different films, and l specifies for each film the number of smectic layers in the thicker areas of the film.

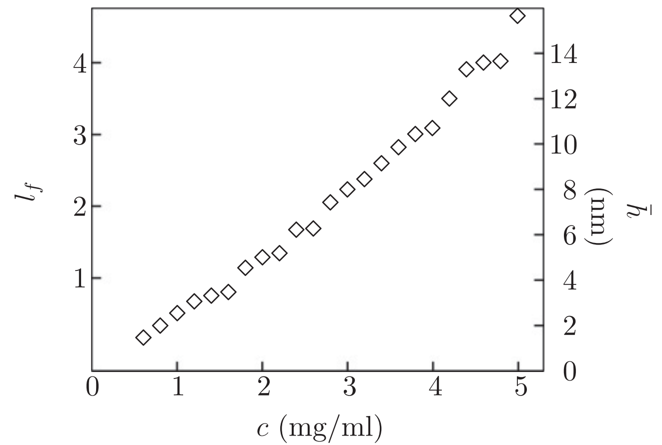

FIG. 4. Dependency of the fractional layer number l_f (see text) and the average film thickness $\bar{h}$ on the 8CB concentration c in the spin-coating solution. The linear relation demonstrates the good controllability of the number of layers and the surface coverage.

obtained for the thicker (film thickness l smectic layers) and the thinner parts (film thickness $l-1$ smectic layers) of a given film. For films obtained with $c < 1.8$ mg/ml, in which the thicker parts consist of the trilayer structure, $\Delta\phi$ is clearly larger than for the thicker films. A large phase difference between different areas of a film indicates that the interactions between the tip and the surface are different in different areas. In our thinnest films ($c < 1.8$ mg/ml), the thicker areas consist of the trilayer structure, and the thinner areas probably consist of an 8CB monolayer or even the bare substrate, and we can expect a larger value of $\Delta\phi$ than in the thicker films, in which the surface is formed by an 8CB bilayer in both the thicker and the thinner areas.

For a more quantitative analysis, the AFM images were binarized; i.e., it was decided whether each pixel belonged to the thicker or thinner part of the film. The transition from the island structure (the thinner areas form a topologically connected space) to the pore structure (the thicker areas are connected) takes place when the incomplete smectic top layer covers ≈35% of the film area. Thus, if we define the porosity of the smectic top layer in analogy to the three-dimensional case as the fraction between the void areas and the total surface, the maximum porosity that could be achieved in our experiments was around 65%.

By determining the area fraction of the smectic top layer from the AFM images of the films, we can assign to each film a fractional layer number l_f and an average thickness $\bar{h}$. For instance, a film with $l_f = 2.75$ would consist, in addition to the tilted monolayer on the substrate, of two complete smectic layers and a top layer that covers 75% of the surface, and its average thickness would be $\bar{h} = 9.63$ nm (4.1 nm for the trilayer structure plus 1.75×3.16 nm for one additional layer and the incomplete top layer). The relation between the 8CB concentration in the spin-coated solution and l_f and $\bar{h}$ is shown in Fig. 4. The data indicate a nearly linear relation between the average film thickness and the 8CB concentration.

Compared to freely suspended films in air and Langmuir films on water, our films possess a more static nature. For instance, in freely suspended and Langmuir films, islands can shrink or relax to a circular shape, whereas in our films islands show an elongated shape [cf. Fig. 1(b)] that does not change. The pores in our films are, on average, more circular, but they also do not change their shape. On the time scale of several hours or 1 day, the AFM images of the prepared films do not show, at ambient temperature, any noticeable change in the surface structure. The different behaviors indicate that the influence of the line tension of the edge of the pores or islands in our films is much smaller than in Langmuir or freely suspended films. This might be one reason why, in Langmuir films, considerably larger (but less numerous) pores are observed [6] compared to our films.

On the time scale of several days, slight changes in the surface structure occur. Figure 5 shows AFM images of a film prepared from a 1 mg/ml solution. The left image was recorded immediately after preparation, and the right image shows the same film area after a period of 5 days. It is obvious that some pores have increased their size and some have "coalesced." The change of the surface structure does not appear to result from a minimization of the line tension of the boundaries separating the thicker and thinner areas; rather, it seems that the thinner parts slowly increase their area and the film experiences a loss of liquid-crystal material from the incomplete top layer.

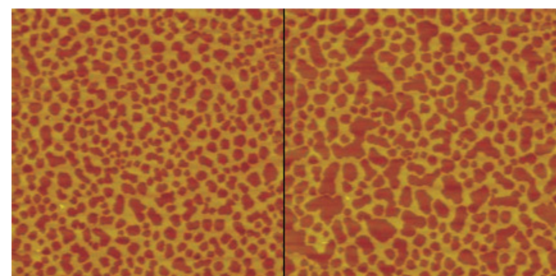

FIG. 5. (Color online) AFM height images (20×20 μm^2) of a film prepared with a 1-mg/ml solution. The left image was recorded immediately after preparation; the right image shows the same area after a period of 5 days.

Within the 5-day period, the fraction of the film surface that is covered by the incomplete top layer decreased from 0.52 to 0.41. Since the film was not stored in a closed atmosphere, a slow evaporation of the 8CB molecules at the edges of the islands or pores might be a possible reason. Despite the static nature of the surface structure, recent studies of the dynamics in ultrathin spin-coated 8CB films have shown that the molecules in these films are still mobile with diffusion coefficients of around 1 $\mu\text{m}^2/\text{s}$ [34].

To confirm the thickness-concentration relation shown in Fig. 4, all prepared films were studied by ellipsometry. The ellipsometric parameters Δ and $\tan\Psi$ were determined as a function of the angle of incidence θ_i within a narrow (a few degrees) interval around the Brewster angle θ_B ($\approx 76.1^\circ$ for a bare silicon wafer). The value of $\tan\Psi$ at $\theta_i = \theta_B$ is commonly designated as ellipticity coefficient $\bar{\rho}$, and its magnitude is almost linearly related to the film thickness h, provided h does not exceed a few tens of nanometers. Usually, h cannot be calculated directly from a measured $\bar{\rho}$ value; instead, one has to compare the experimental $\bar{\rho}$ values with calculated $\bar{\rho}$ values resulting from a model system. The calculation of $\bar{\rho}$ for model systems consisting of an arbitrary number of possibly anisotropic layers between two semi-infinite bulk media can be done using the 4×4 matrix method [35,36]; an example for freely suspended smectic films is given in [37]. In our case, we use the simple model system sketched in Fig. 6, consisting of the silicon wafer (refractive index $n = 4.05 - i0.028$), a thin silicon oxide layer ($n = 1.47$), a uniaxial birefringent layer possessing the optical properties of 8CB ($n_o = 1.51$, $n_e = 1.67$ [38,39], optical axis parallel to film normal), and air ($n = 1$). The introduction of a tilt of the optical axis in a 1-nm-thick sublayer of the birefringent layer (in order to mimic the tilted monolayer on the substrate surface) would change the calculated $\bar{\rho}$ values by less than 1.5%, which is beyond our experimental resolution. We have therefore neglected a tilted layer in our model. For a bare silicon wafer with a native silicon oxide layer we measure $\bar{\rho} = 0.02$; this value is reproduced by our model if we set the thickness of the SiO_2 layer to 1.6 nm. Using this value, we have calculated $\bar{\rho}$ as a function of the thickness of the birefringent layer, leading to the result shown in Fig. 6.

Obviously, our simple model neglects the island or pore structure at the air interface of our films. However, the film area probed by the laser beam of the ellipsometer amounts to ≈ 1 mm^2, whereas the length scale of the islands and pores is in the micron range; i.e., our ellipsometer just sees an average surface roughness. We could take this into account in our model by replacing the sharp jump of the refractive indices at the film-air interface by a continuous refractive index profile, usually described by a tanh function. If we consider, e.g., a film with an incomplete smectic top layer that covers, say, 50% of the film area, in our model, we would have to replace a 1.6-nm-thick birefringent layer with a sharp air interface with a 3.2-nm-thick birefringent layer in which n_o and n_e vary continuously between the values of 8CB and the value of air. However, when we calculate the value of $\bar{\rho}$ for both models we find that the difference in $\bar{\rho}$ is of the order 0.005 (corresponding, in the simpler model, to a thickness change of 0.3 nm) and is thus at the edge of our experimental resolution.

Using the calculated relation between $\bar{\rho}$ and h shown in Fig. 6, we have assigned a thickness value to the measured $\bar{\rho}$ value of each film. The result is shown in Fig. 7, together with the thickness data determined from the AFM measurements. Both thickness data sets coincide well; i.e., the ellipsometry data provide a strong confirmation of the AFM measurements.

We have also conducted preliminary thermal studies of these films. The films with $l_f \leqslant 1$ can be heated to a temperature of 58 °C without noticeable structural changes in the AFM images. At higher temperatures, the steps associated with the pores vanish, and the formation of droplets is observed, i.e., the films start to dewet. The same process can be observed for the films with $1 < l_f \leqslant 2$ at about 38 °C and for the films with $2 < l_f \leqslant 3$ at about 37 °C. Comparison with the bulk transition temperatures of 8CB (smectic-A 33.7 °C nematic 40.5 °C isotropic) clearly shows that the smectic layer structure is strongly stabilized in these ultrathin films. The droplets, which have been formed at higher temperatures, start

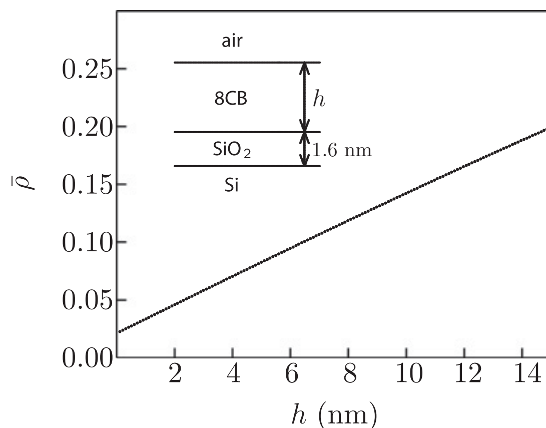

FIG. 6. Calculated values of the ellipticity coefficient $\bar{\rho}$ as function of the thickness h of a uniaxial birefringent film on a silicon wafer with a 1.6-nm-thick native oxide layer. The refractive indices of the birefringent film were set to the values determined for 8CB (see text); the optical axis was assumed to be parallel to the film normal.

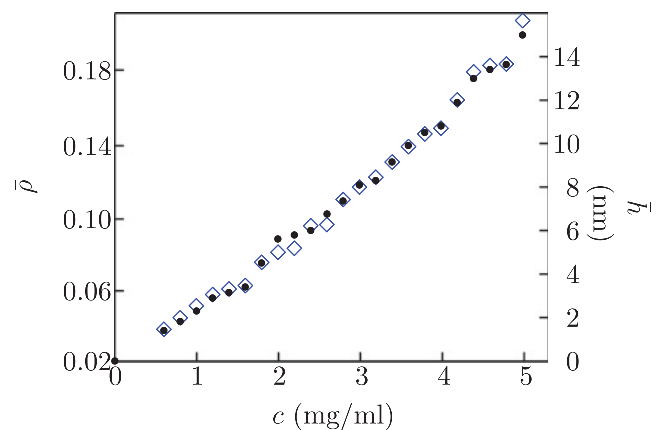

FIG. 7. (Color online) Measured values (dots) of the ellipticity coefficient $\bar{\rho}$ as a function of the 8CB concentration c in the spin-coating solution; the right-hand scale gives the average film thickness $\bar{h}$ resulting from the ellipsometry data. The blue diamonds are the $\bar{h}$ values resulting from the AFM measurements (same data as shown in Fig. 4).

to spread on the substrate when the temperature is decreased again to the smectic range. However, the dewetting process can proceed in an inhomogeneous way over the film. For example, for the films with $1 < l_f \leqslant 2$ the first small droplets can be already observed at a temperature of 33 °C, although most parts of the film remain stable several degrees above this value even after an equilibration time of 1 day. We tentatively assign the dewetting at lower temperatures to the formation of droplets induced by impurities on the substrate surface, whereas the higher temperatures might correspond to the behavior on a smooth silicon wafer.

In future studies, the ultrathin films described here might be used as model systems for two-dimensional porous diffusion. If we assume that the molecules of the tilted monolayer are adsorbed on the substrate surface (in a similar way as observed for 8CB on graphite [40] and molybdenum disulfide [41]) and do not participate in the diffusion process, porous films with $l_f \leqslant 1$ would look for a diffusing molecule as a real porous medium, and the diffusion itself would be perfectly two-dimensional. Single-molecule fluorescence studies [34] would provide a possible method for quantitative diffusion measurements in these systems.

IV. CONCLUSIONS

We studied ultrathin smectic films of the compound 8CB, spin coated from solution onto silicon substrates. By controlling the concentration of 8CB in the spin-coating solution, we could prepare films with a defined small number (between one and four) of smectic layers. Using AFM measurements, we have shown that the films possess a specific surface structure with a lateral feature size of a few microns and steplike height variations of 3.3 nm. The height of the steps corresponds to the smectic layer spacing in the volume smectic-A_d phase of 8CB, indicating that the surface structure is the result of a partial formation of the topmost smectic layer of the films: unless the 8CB concentration c in the spin-coating solution is precisely tuned to certain values, the topmost smectic layer of the films is either fragmented to isolated islands or shows a porous structure. When c is stepwise increased starting from zero, first, isolated islands appear that then merge to a porous structure, and finally, at $c \approx 1.8$ mg/ml, a film with a smooth surface is obtained. Ellipsometry shows that this first "complete" film possesses the same thickness as the well-known [5,13,19,20] trilayer structure that is formed by 8CB on polar substrates with planar anchoring conditions. Further increasing c leads again to the structural island-pore sequence until the next smectic layer is completed. The values of the step height at the edge of the pores or islands indicate that the smectic layers that form in thicker films on top of the trilayer possess the same thickness as the smectic layers in the volume smectic phase of 8CB; i.e., it is likely that they possess the same bilayer structure of interdigitating molecules. Preliminary thermal studies have indicated a strongly enhanced stability of the smectic layer structure in the ultrathin films. Ellipsometric measurements of the total average film thickness confirmed the structures resulting from the AFM measurements. Our study is also the first demonstration of the preparation of smectic 8CB films on silicon with a thickness of two, three, or four smectic layers. In principle, this is also possible by spontaneous spreading of 8CB but would require weeks for the reported spreading rate of 2–3 nm/s [21]; in an evaporation experiment [13], it was not possible to obtain homogeneous 8CB films with a thickness larger than the trilayer structure (which contains just one volume-like smectic layer).

We have demonstrated that there is a well-defined relation between the 8CB concentration in the spin-coating solution and the resulting surface structure, thereby enabling the targeted generation of island structures or pore structures, the porosity of which can be, to a certain extent, tuned quantitatively. In future studies, our films might be of interest for the controlled preparation of quasi-two-dimensional porous soft-matter systems.

ACKNOWLEDGMENT

Stimulating discussions with Stephan Herminghaus are gratefully acknowledged.

[1] P. Pieranski, L. Beliard, J.-Ph. Tournellec, X. Leoncini, C. Furtlehner, H. Dumoulin, E. Riou, B. Jouvin, J.-P. Fénerol, Ph. Palaric, J. Heuving, B. Cartier, and I. Kraus, Phys. A **194**, 364 (1993).

[2] J.-C. Géminard, R. Holyst, and P. Oswald, Phys. Rev. Lett. **78**, 1924 (1997).

[3] P. Oswald, F. Picano, and F. Caillier, Phys. Rev. E **68**, 061701 (2003).

[4] B. Rapp and H. Gruler, Phys. Rev. A **42**, 2215 (1990).

[5] J. Xue, C. S. Jung, and M. W. Kim, Phys. Rev. Lett. **69**, 474 (1992).

[6] M. C. Friedenberg, G. G. Fuller, C. W. Frank, and C. R. Robertson, Langmuir **10**, 1251 (1994).

[7] M. N. G. de Mul and J. A. Mann, Langmuir **10**, 2311 (1994).

[8] L. Zou, J. Wang, P. Basnet, and E. K. Mann, Phys. Rev. E **76**, 031602 (2007).

[9] A. Hochbaum and M. M. Labes, J. Appl. Phys. **53**, 2998 (1982).

[10] M. Woolley, R. H. Tredgold, and P. Hodge, Langmuir **11**, 683 (1995).

[11] A. Itaya, K. Watanabe, T. Imamura, and H. Miyasaka, Thin Solid Films **292**, 204 (1997).

[12] M. Bardosova, I. Clarke, P. Hodge, R. H. Tredgold, and M. Woolley, Thin Solid Films **300**, 234 (1997).

[13] I. D. Drevenšek Olenik, K. Kočevar, I. Muševič, and Th. Rasing, Eur. Phys. J. E **11**, 169 (2003).

[14] E. Olbrich, O. Marinov, and D. Davidov, Phys. Rev. E **48**, 2713 (1993).

[15] M. W. J. van der Wielen, M. A. Cohen Stuart, G. J. Fleer, D. K. G. de Boer, A. J. G. Leenaers, R. P. Nieuwhof, A. T. M. Marcelis, and E. J. R. Sudhölter, Langmuir **13**, 4762 (1997).

[16] E. Lacaze, J. P. Michel, M. Goldmann, M. Gailhanou, M. de Boissieu, and M. Alba, Phys. Rev. E **69**, 041705 (2004).

[17] J. P. Michel, E. Lacaze, M. Alba, M. de Boissieu, M. Gailhanou, and M. Goldmann, Phys. Rev. E **70**, 011709 (2004).
[18] R. Garcia, E. Subashi, and M. Fukuto, Phys. Rev. Lett. **100**, 197801 (2008).
[19] J. Daillant, G. Zalczer, and J. J. Benattar, Phys. Rev. A **46**, 6158 (1992).
[20] S. Bardon, R. Ober, M. P. Valignat, F. Vandenbrouck, A. M. Cazabat, and J. Daillant, Phys. Rev. E **59**, 6808 (1999).
[21] L. Xu, M. Salmeron, and S. Bardon, Phys. Rev. Lett. **84**, 1519 (2000).
[22] R. Lucht and Ch. Bahr, Phys. Rev. Lett. **85**, 4080 (2000).
[23] B. Zappone and E. Lacaze, Phys. Rev. E **78**, 061704 (2008).
[24] J. Maclennan, G. Decher, and U. Sohling, Appl. Phys. Lett. **59**, 917 (1991).
[25] R. M. Overney, E. Meyer, J. Frommer, H.-J. Güntherodt, G. Decher, J. Reibel, and U. Sohling, Langmuir **9**, 341 (1993).
[26] I. V. Chikina, N. Limodin, A. Langlois, M. Brazovskaia, C. Even, and P. Pieranski, Eur. Phys. J. B **3**, 189 (1998).
[27] M. Tarabia, G. Cohen, D. Davidov, and C. Escher, Ferroelectrics **149**, 35 (1993).
[28] M. Tarabia, G. Cohen, J. Gersten, and D. Davidov, Phys. Rev. E **51**, 799 (1995).
[29] W. Guo, S. Herminghaus, and Ch. Bahr, Langmuir **24**, 8174 (2008).
[30] R. Lucht, Ch. Bahr, and G. Heppke, Phys. Rev. E **62**, 2324 (2000).
[31] A. J. Leadbetter, J. C. Frost, J. P. Gaughan, G. W. Gray, and A. Mosley, J. Phys. (Paris) **40**, 375 (1979).
[32] G. W. Gray and J. E. Lydon, Nature (London) **252**, 221 (1974).
[33] S. Bardon, M. P. Valignat, and A. M. Cazabat, Langmuir **14**, 2916 (1998).
[34] B. Schulz, D. Täuber, F. Friedriszik, H. Graaf, J. Schuster, and C. von Borczyskowski, Phys. Chem. Chem. Phys. **12**, 11555 (2010).
[35] S. Teitler and B. Henvis, J. Opt. Soc. Am. **60**, 830 (1970).
[36] D. W. Berreman, J. Opt. Soc. Am. **62**, 502 (1972).
[37] D. Schlauf, Ch. Bahr, V. K. Dolganov, and J. W. Goodby, Eur. Phys. J. B **9**, 461 (1999).
[38] P. P. Karat and N. V. Madhusudana, Mol. Cryst. Liq. Cryst. **36**, 51 (1976).
[39] R. G. Horn, J. Phys. (Paris) **39**, 105 (1978).
[40] D. P. E. Smith, J. K. H. Hörber, G. Binnig, and H. Nejoh, Nature (London) **344**, 641 (1990).
[41] M. Hara, Y. Iwakabe, K. Tochigi, H. Sasabe, A. F. Garito, and A. Yamada, Nature (London) **344**, 228 (1990).